Vapor-Liquid Equilibria of Light Hydrocarbons at Low Temperatures and High Pressures:
The Methane-*n*-Heptane System

HARRY L. CHANG, LEWIS J. HURT, and RIKI KOBAYASHI
Rice University, Houston, Texas

Recent experimental observations of the phase behavior of methane–*n*-paraffin hydrocarbon binary systems are used to make a phase rule analysis of such systems. The vapor-liquid equilibria of light hydrocarbon systems are complicated by liquid-liquid immiscibility and solids formation at low temperatures.

The system studied here has limited liquid phase miscibility with a quadruple point involving a gas phase, two liquid phases, and a solid phase.

Experimental techniques were developed to sample and analyze gas phases containing concentrations of *n*-heptane in the range of 0.00001 mole fraction with good precision. Binary *K* values for methane and *n*-heptane are reported at intervals of 20°F. from 0° to —100°F. for pressures up to the criticals for the mixtures. The results are reported numerically and illustrated graphically. Additional phase observations were made below the critical temperature of methane to confirm and extend the phase behavior of the methane–*n*-heptane system as reported by Kohn.

Since the review of the vapor-liquid equilibria of light hydrocarbons at low temperatures by Price and Kobayashi (*12*), studies on the phase behavior of the methane–*n*-hexane (*4*), methane–*n*-heptane (*5*), and methane–*n*-octane (*6*) systems by Kohn and co-workers have appeared. The methane–*n*-decane systems were reported by Stalkup et al. (*17*) and also studied by Koonce and Kobayashi (*7*). Koonce et al. (*8*) reported vapor-liquid equilibria data on the ternary methane–propane–*n*-decane and the methane–propane–*n*-heptane systems in 1965.

GENERAL DISCUSSION OF PHASE BEHAVIOR IN METHANE–*n*-PARAFFIN HYDROCARBON BINARIES

The experimental results reported by Kohn (*5, 6*) and by Stalkup and Kobayashi (*17*) and in this paper indicate that the binary phase behavior of methane with other *n*-paraffin hydrocarbons through *n*-decane offers at least three types of phase behavior:

1. Systems in which the critical locus runs continuously from the critical of pure methane to the critical of the higher boiling constituent with complete liquid phase miscibility.
2. Systems in which the critical locus runs from the critical of the higher boiling constituent to a liquid-liquid critical locus occurring at a temperature below the critical temperature of pure methane and at a pressure considerably in excess of the critical for pure methane; that is, when a liquid-liquid-solid-gas quadruple point occurs in the binary system.
3. Systems in which the critical locus starting from the critical of the heavier component is severed by the intrusion of the solid-liquid-gas phase relationship upon the vapor-liquid equilibrium region, giving a second critical locus which extends from the critical point of pure methane to a gas-liquid critical point with solids present.

These three types of systems are exemplified by the pressure-temperature projection of the methane-propane, methane–*n*-heptane, and methane–*n*-decane systems, respectively, as shown in Figures 1, 2, and 3.

It has been verified experimentally that the binary systems of methane with ethane (*11, 12*) and *n*-butane (*9, 16*) are qualitatively similar to those of the methane-propane system. The liquid phase miscibility was complete over the entire composition range and the critical locus runs continuously from the critical of pure methane to the heavier component.

An example of the second type of system is the methane–*n*-heptane system whose pressure-temperature projection has been developed from the data of Kohn (*5*) and the authors of this work and are presented in Figure 2.

Lewis J. Hurt is at Rohm and Haas Company, Huntsville, Alabama.

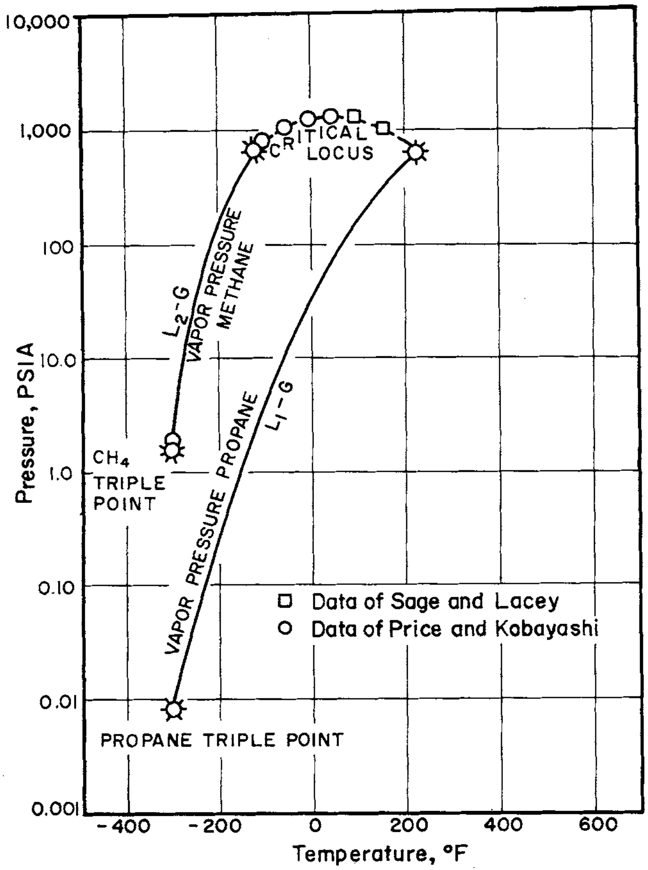

Fig. 1. Pressure-temperature projection for the methane-propane system.

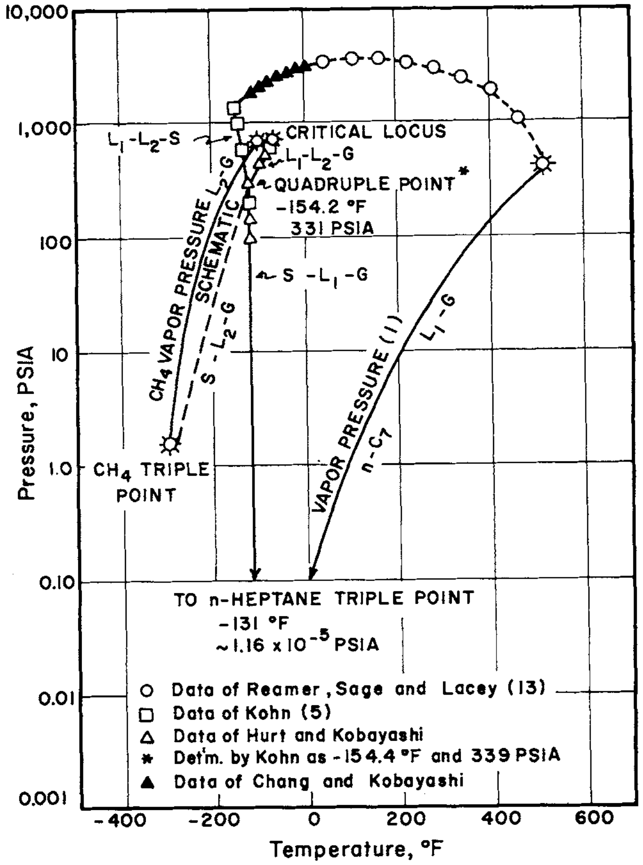

Fig. 2. Pressure-temperature projection for the methane–*n*-heptane system.

This system is characterized by liquid-liquid immiscibility and a quadruple point involving two liquid phases, a gas phase, and solid *n*-heptane phase. The four three-phase lines emanating from the quadruple point are L_1-L_2-S, L_1-L_2-G, L_1-S-G, and L_2-S-G. The $L_1 \equiv G$ critical locus runs from the critical of pure *n*-heptane to the three phase critical in which the intensive properties of the two liquid phases become identically equal ($L_1 \equiv L_2$) with solid *n*-heptane present. The phase behavior indicates that $L_1 = G$ critical locus is considerably higher in pressure than would be the case if the critical loci ran from that of pure *n*-heptane to pure methane. This behavior implies that the compositional effects of intermediate components such as ethane, propane, or *n*-butane on the K values are considerably more pronounced than estimated from the convergence pressure concept (2).

The third type of methane–*n*-paraffin binary system is exemplified by the methane–*n*-decane and the methane–*n*-octane systems (6). Figure 3 is a schematic pressure-temperature projection of the methane–*n*-decane system showing the solid-liquid-gas features intersecting the critical locus of *n*-decane to terminate one branch of the $L_1 = G$ critical locus. We postulate that a second branch of the critical locus falls in the vicinity of the pure methane critical point. Two requirements for this type of system are: (1) that the freezing point of the heavier component be lowered only slightly by the solution of methane in the heavier hydrocarbon, and (2) that the triple point of the heavier hydrocarbon be considerably higher in temperature than the critical point of methane. On the basis of known binary methane–*n*-paraffin systems, it may be concluded that all binary mixtures of methane and *n*-paraffins of molecular weight equal to or greater than *n*-octane fall into this category (6).

A schematic temperature-composition diagram for the methane–*n*-decane system at a constant pressure in the

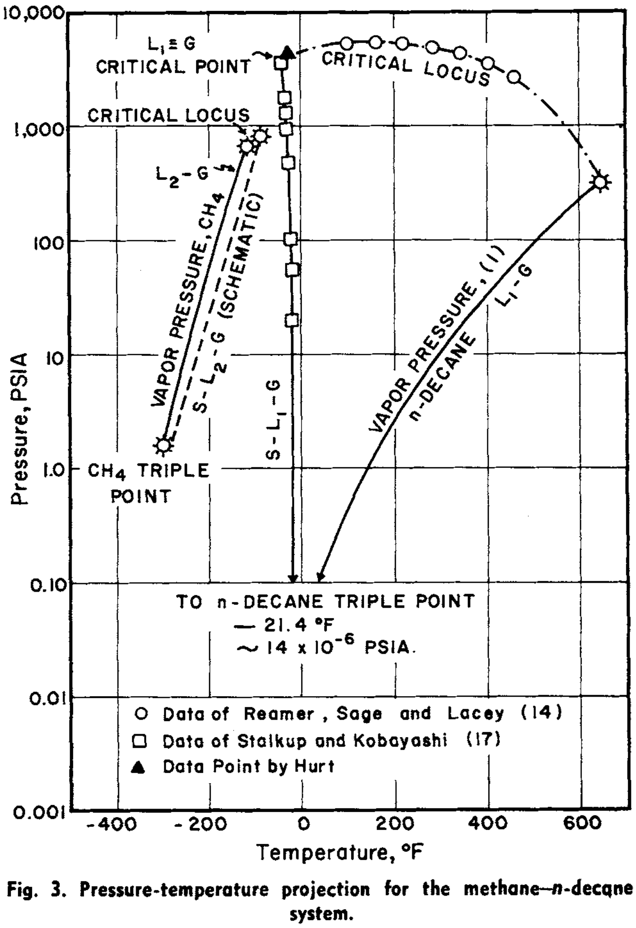

Fig. 3. Pressure-temperature projection for the methane–*n*-decqne system.

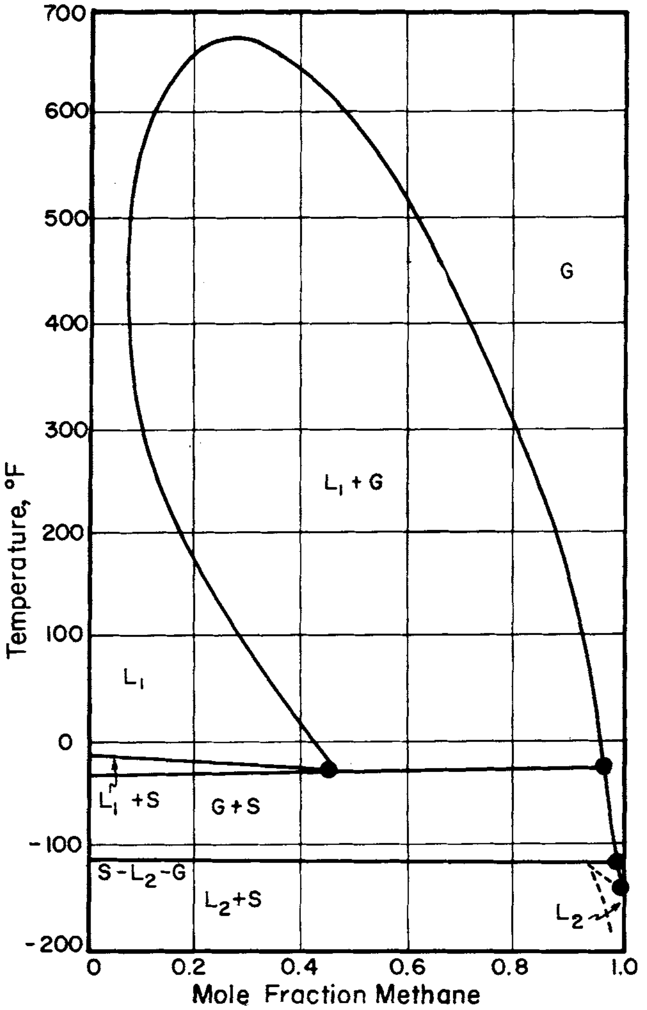

Fig. 4. Schematic temperature composition diagram of the methane–*n*-decane binary at 500 lb./sq.in.abs.

TABLE 1. EXPERIMENT RANGE OF PRESSURE AND TEMPERATURES STUDIED

Temperature, °F.	Pressure range, lb./sq. in. abs.
0	100 to 3,000
—20	100 to 2,750
—40	100 to 2,500
—60	100 to 2,250
—80	100 to 2,000
—100	100 to 1,750

TABLE 2. OBSERVED CRITICAL PRESSURES OF METHANE-*n*-HEPTANE

Temperature, °F.	Pressure, lb./sq. in. abs.
0	3,042
—20	2,864
—40	2,655
—60	2,435
—80	2,200
—100	1,948
—114	1,803

neighborhood of 500 lb./sq. in. abs. is presented in Figure 4.

EXPERIMENTAL EQUIPMENT

The experimental equipment used in this investigation was of the vapor recycle type described by Price and Kobayashi (*12*). Several significant changes in the original apparatus have been made to permit proper equilibration and sampling of mixtures of such widely boiling components as methane and *n*-heptane.

First, a magnetic vapor recycling pump mounted entirely within the low temperature bath was developed. In this way, the cold recycle vapors were never permitted to leave the bath, thus eliminating any possibilities of forming a two-phase condition outside of the equilibrium cell. A compound bar magnet was raised and lowered mechanically to actuate the soft iron plunger, producing an essentially isothermal pumping operation.

Second, the sampling leads were made of a 1/16-in. O.D. by 0.019-in. I.D. stainless steel capillary tubing which directly connected to the chromatographic analyzing unit. Upon leaving the equilibrium cell, the sample was immediately reduced to a pressure below atmospheric through a needle valve. The insulated, heated sampling tubing was maintained at a temperature of approximately 300°F. by means of nichrome heating wire to insure complete conversion of the sample to a single phase gaseous state before it entered the sample loop of the flame ionization chromatography unit.

Refrigeration for the runs made at temperatures down to — 100°F. was provided by a two-stage, air-cooled condensing refrigeration unit assembled from commercial units. For the exploratory phase behavior runs, liquid nitrogen refrigeration was used. Temperature was controlled by a heater connected to an on-off electronic thermal regulator. A ten-junction thermopile with the Leeds & Northrup millivolt potentiometer was used to measure the temperature. The thermopile was calibrated against a platinum resistance thermometer with a K-3 Leeds & Northrup potentiometer. Temperature fluctuations during calibration and the experimental runs were found to be less than ∓ 0.01°F. System pressure was controlled by means of a positive displacement mercury pump connected to the system through a stainless steel bomb which was also used as a methane reservoir. The system pressure could be maintained to within ± 1 lb./sq.in. of the desired operating condition. The pressure was indicated with two calibrated Heise gauges of ranges from 0 to 2,000 lb./sq.in. and 0 to 10,000 lb./sq.in. These gauges were certified to have maximum hysteresis of ± 1.0 and ± 2.0 lb./sq.in., respectively, by the manufacturers.

ANALYTICAL PROCEDURE

The analytical equipment consisted of a commercial chromatograph with a flame ionization detector and an electrometer. A 5-ft. 5-in. by ⅛-in. O.D. column, packed with 20 wt. % Dow Corning 200/500 on acid-washed firebrick, was utilized to separate the components. The column was maintained at 220°F. and operated with a helium flow rate of 15 cc./min. The chromatograms were recorded and integrated with an electronic integrator which had a reproducibility of 0.1% of the full-scale value. A gravimetric method was used to pre-

TABLE 3. OBSERVED THREE- AND FOUR-PHASE CONDITIONS OF THE METHANE-*n*-HEPTANE SYSTEM

Phases	Temperature, °F.	Pressure, lb./sq. in. abs.
L_1L_2G	—126.0	570
L_1L_2G	—130.0	519
L_1L_2G	—140.0	435
SL_2G	—139.5	98
SL_2G	—136.7	155
SL_1L_2G	—154.2	331
Type K singular point[*]	—114.7	694

[*] Type K singular point as defined by Ricci (*15*).

TABLE 4. VAPOR-LIQUID EQUILIBRIUM DATA OF THE METHANE-*n*-HEPTANE BINARY

Temp., °F.	Press., lb./sq. in. abs.	Vapor mole % *n*-heptane	Liquid mole % *n*-heptane	K values K_1	K_7
0	100	0.143	95.550	22.44	0.00150
0	200	0.123	90.988	11.08	0.00135
0	400	0.104	82.559	5.73	0.00126
0	600	0.127	75.096	4.01	0.00169
0	800	0.140	68.400	3.16	0.00205
0	1,000	0.162	62.280	2.64	0.00261
0	1,250	0.222	55.479	2.24	0.00400
0	1,500	0.361	50.343	2.00	0.00717
0	1,750	0.416	44.300	1.78	0.00939
0	2,000	0.573	38.307	1.60	0.01496
0	2,250	0.735	33.410	1.48	0.02110
0	2,500	1.465	28.169	1.36	0.05201
0	2,750	2.660	22.112	1.24	0.12030
0	3,000	6.001	14.150	1.09	0.42410
—20	100	0.064	95.097	20.38	0.00067
—20	200	0.055	89.670	9.68	0.00061
—20	400	0.066	81.170	5.31	0.00081
—20	600	0.076	73.315	3.74	0.00104
—20	800	0.091	65.875	2.93	0.00138
—20	1,000	0.107	59.219	2.45	0.00181
—20	1,250	0.151	52.159	2.09	0.00289
—20	1,500	0.211	46.115	1.85	0.00458
—20	1,750	0.293	39.415	1.64	0.00743
—20	2,000	0.404	33.417	1.49	0.01209
—20	2,250	0.696	27.810	1.37	0.02503
—20	2,500	1.167	21.873	1.27	0.05335
—20	2,750	2.440	13.660	1.13	0.17862
—40	100	0.030	94.445	18.00	0.00032
—40	200	0.026	88.368	8.60	0.00029
—40	400	0.032	79.190	4.80	0.00040
—40	600	0.042	70.099	3.34	0.00060
—40	800	0.052	62.720	2.68	0.00083
—40	1,000	0.067	55.191	2.23	0.00121
—40	1,250	0.093	48.404	1.94	0.00192
—40	1,500	0.131	42.105	1.73	0.00311
—40	1,750	0.182	34.512	1.52	0.00527
—40	2,000	0.254	26.254	1.35	0.00967
—40	2,250	0.400	18.501	1.22	0.02162
—40	2,500	0.800	11.201	1.12	0.07142
—60	100	0.015	93.720	15.92	0.00016
—60	200	0.013	87.650	8.10	0.00015
—60	400	0.015	76.780	4.31	0.00020
—60	600	0.020	67.450	3.07	0.00030
—60	800	0.027	58.830	2.43	0.00046
—60	1,000	0.036	50.790	2.03	0.00071
—60	1,250	0.049	42.800	1.75	0.00115
—60	1,500	0.071	34.580	1.53	0.00105
—60	1,750	0.095	27.200	1.37	0.00349
—60	2,000	0.146	20.510	1.26	0.00712
—60	2,250	0.341	11.810	1.14	0.02790
—80	100	0.0070	92.740	13.77	0.000075
—80	200	0.0068	85.910	7.10	0.000079
—80	400	0.0080	73.700	3.80	0.000110
—80	600	0.0100	62.200	2.65	0.000160
—80	800	0.0146	52.350	2.09	0.000290
—80	1,000	0.0206	44.510	1.80	0.000470
—80	1,250	0.0280	35.200	1.54	0.000800
—80	1,500	0.0410	27.900	1.39	0.001470
—80	1,750	0.0780	19.700	1.24	0.003960
—80	2,000	0.1410	10.890	1.12	0.012950
—100	100	0.0036	91.530	11.81	0.000039
—100	200	0.0036	83.650	6.12	0.000043
—100	400	0.0045	68.900	3.22	0.000070
—100	600	0.0060	53.880	2.17	0.000110
—100	800	0.0090	43.480	1.77	0.000210
—100	1,000	0.0140	37.600	1.60	0.000370
—100	1,250	0.0200	28.500	1.40	0.000700
—100	1,500	0.0300	19.440	1.24	0.001540
—100	1,750	0.0700	10.000	1.11	0.007000

pare samples of known composition for calibration of the flame ionization detector. In this way, the mole fractions of each components were obtained to an error of less than 0.05%. The sample bombs were mixed by introducing severe thermal gradients in the sample container. A heating period of approximately 24 hr. was used to insure homogeneous samples. Samples of these known mixtures were introduced into the sample loop through a 1/16-in. O.D. and 0.019-in. I.D. stainless steel tubing which was also heated to a temperature of approximately 300°F. The subsequent chromatograms were then recorded and integrated. The mole fractions of the components were then obtained by using a calibration factor which had been obtained by analyzing known mixtures.

Due to the high sensitivity of the flame ionization detector, it was possible to detect, record, and integrate the *n*-heptane chromatograms for *n*-heptane down to 0.001 mole % with a relative accuracy less than 5% of the amount present at the lowest concentrations.

The maximum error in the determination of the *n*-heptane in the vapor phase was established in the following manner:

1. Percentage error of the area factor f

$$f = \frac{x_1}{x_7}\cdot\frac{A_7}{A_1} \qquad (1)$$

where x_1, x_7 are the mole fractions of methane and *n*-heptane and A_1, A_7 are the peak areas of methane and *n*-heptane.

$$df = \frac{\partial f}{\partial x_1}dx_1 + \frac{\partial f}{\partial x_7}dx_7 + \frac{\partial f}{\partial A_1}dA_1 + \frac{\partial f}{\partial A_7}dA_7 \qquad (2)$$

$$\Delta f = \frac{\partial f}{\partial x_1}\Delta x_1 + \frac{\partial f}{\partial x_7}\Delta x_7 + \frac{\partial f}{\partial A_1}\Delta A_1 + \frac{\partial f}{\partial A_7}\Delta A_7 \qquad (3)$$

$$\frac{\Delta f}{f} = \frac{\Delta A_1}{A_1} + \frac{\Delta A_7}{A_7} + \frac{\Delta x_1}{x_1} + \frac{\Delta x_7}{x_7} \qquad (4)$$

For a known mixture of $x_1 = 0.98883$ and $x_7 = 0.01117$, we obtain $A_1 = 3.54$ $A_7 = 0.26$; hence $f = \frac{x_1A_7}{x_7A_1} = 6.6018$. The probable error of A caused by electrometer and integrator recorder is 0.2% and the mole fractions error is 0.05% due to the preparation of known mixtures.

Therefore $\frac{\Delta f}{f} = 0.2\% + 0.2\% + 0.05\% + 0.05\% = 0.5\%$.

2. Percentage error of x_7

$$x_7 = \frac{A_7}{f_1 A_1 + A_7}$$

$$\frac{\Delta x_7}{x_7} = \frac{f}{(fA_1 + A_7)A_7}(A_1\,\Delta A_7 + A_7\cdot\Delta A_1 + A_7\cdot\Delta f) \qquad (5)$$

which was derived in the same manner as in 1. In analyzing an unknown sample it was found that $A_1 = 105.32$, $A_7 = 0.22$, and $f = 6.6018$ for $A_1 >> A_7$ and for the range of concentration studied, the maximum probable error caused by the electrometer and integrator recorder is ± 3%; the error in A_1 is still 0.2% and $\Delta f/f = 0.5\%$. By substituting these known values into Equation (5) we obtain $(\Delta x_7/x_7) = 3.23\%$, which is the maximum percentage error of the mole fraction of *n*-heptane in the vapor phase. The corresponding concentration of *n*-heptane in the vapor phase was 0.000317. From a multitude of similar calculations, the maximum percentage error of the *n*-heptane in the concentration in the vapor phase was found to be less than 5% of the amount present.

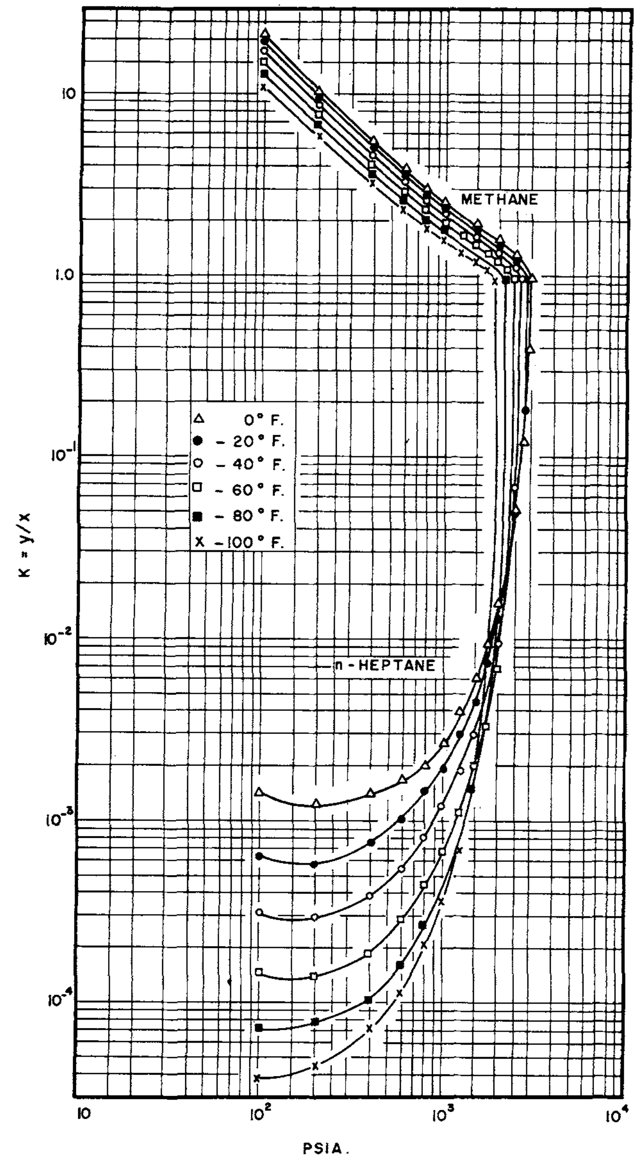

Fig. 5. *K* value vs. pressure for methane–*n*-heptane system.

EXPERIMENTAL RESULTS AND DISCUSSION

Equilibrium measurements were made on a large number of mixtures involving methane and *n*-heptane over the temperature and pressure conditions given in Table 1.

Tables 2 and 3 present a tabulation of the critical loci and the observed three- and four-phase conditions of the methane–*n*-heptane system. Table 4 presents a complete tabulation of all binary phase composition data determined in this investigation, together with the graphically smoothed methane and *n*-heptane *K* values. Plots of *K* value vs. pressure for the isotherms studied are presented in Figure 5. It is observed that the Raoult-Dalton relationships do not hold for this system at any of the experimental conditions encountered in this investigation, and the deviations are probably significant even at 1 atm. pressure for the lower temperatures.

A comparison of the experimentally determined *K* values with the Natural Gas Processors Association (NGPA) values is made in Tables 5 and 6. The NGPA values correspond to the *K* values with 3,000 lb./sq. in. abs. convergence pressure at a temperature of —40°F. The experimental convergence pressure at this temperature was 2,864 lb./sq. in. abs. Additional comparisons of K_{exp} vs. K_{NGPA} have been reported elsewhere (*3*).

TABLE 5. METHANE *K* VALUES, *T* = —40°F.

Pressure, lb./sq. in. abs.	K_{NGPA} (*10*), 3,000 lb./sq. in. abs. conv. press.	$K_{exp.}$	$K_{NGPA}/K_{exp.}$
100	15.00	18.00	0.834
200	7.20	8.60	0.839
600	2.26	3.34	0.678
1,000	1.75	2.23	0.785
2,000	1.20	1.35	0.889

TABLE 6. *n*-HEPTANE *K* VALUES, *T* = —40°F.

Pressure, lb./sq. in. abs.	K_{NGPA} (*10*), 3,000 lb./sq. in. abs. conv. press.	$K_{exp.}$	$K_{NGPA}/K_{exp.}$
100	0.00027	0.00032	0.84
200	0.00023	0.00029	0.80
600	0.00030	0.00060	0.50
1,000	0.00053	0.00121	0.44
2,000	0.00410	0.00967	0.42

ACKNOWLEDGMENT

The authors gratefully acknowledge the financial support of Brown and Root, Inc., and the Natural Gas Processors Association. The Dow Chemical Company provided a fellowship during the earlier stages of the work. High purity methane was supplied by Associated Oil and Gas Company and the research grade *n*-heptane was provided by Phillips Petroleum Company.

LITERATURE CITED

1. "Selected Values of Physical and Thermodynamic Properties of Hydrocarbons and Related Compounds," API Project 44, Carnegie Press (1953).
2. Hadden, S. T., *Chem. Eng. Progr. Symposium Ser. No. 7*, **49**, 53 (1953).
3. Kobayashi, Riki, H. L. Chang, and L. D. Van Horn, Proc. Forty Fifth Ann. Convention NGPA, Denver, Colo. (1966).
4. Kohn, J. P., and J. Shim, *J. Chem. Eng. Data*, **7**, 3 (1962).
5. Kohn, J. P., *A.I.Ch.E. J.*, **7**, 514 (1961).
6. ———, and W. F. Bradish, *J. Chem. Eng. Data*, **9**, 5 (1964).
7. Koonce, K. T., and Riki Kobayashi, *ibid.*, 490.
8. Koonce, K. T., H. A. Deans, and Riki Kobayashi, *A.I.Ch.E. J.*, **11**, 259 (1965).
9. McKetta, J. J., L. R. Roberts, R. H. Wang, and A. Azarnoosh, *J. Chem. Eng. Data*, **7**, 484 (1962).
10. "NGAA Equilibrium Ratio Data Book," NGAA, Tulsa, Okla. (1957).
11. Price, A. R., Ph.D. thesis, Rice Univ., Houston, Tex. (1957).
12. ———, and Riki Kobayashi, *J. Chem. Eng. Data*, **4**, No. 1, 40 (1958).
13. Reamer, H. H., B. H. Sage, and W. N. Lacey, *Chem. Eng. Data Ser.*, **1**, 29 (1956).
14. Reamer, H. H., B. H. Sage, and W. N. Lacey, *Ind. Eng. Chem.*, **42**, 534 (1950).
15. Ricci, J. E., "The Phase Rule and Heterogeneous Equilibrium," Nostrand, New York (1951).
16. Shearer, L. T., and Riki Kobayashi, unpublished data.
17. Stalkup, Fred I., and Riki Kobayashi, *A.I.Ch.E. J.*, **9**, 121 (1963).

Manuscript received March 10, 1966; revision received June 3, 1966; paper accepted June 6, 1966.